

STANDARD SOLAR MODELS IN THE LIGHT OF NEW HELIOSEISMIC CONSTRAINTS II. MIXING BELOW THE CONVECTIVE ZONE

A. S. BRUN^{1,2}, S. TURCK-CHIEZE

¹DSM/DAPNIA/Service d'Astrophysique, CEA Saclay, 91191 Gif-sur-Yvette, France

AND

J. P. ZAHN

²Département d'Astrophysique Stellaire et Galactique, Observatoire de Paris, Section Meudon,
92195 Meudon, France

Received 1999 March 2 ; accepted 1999 April 26

ABSTRACT

In previous work, we have shown that recent updated standard solar models cannot reproduce the radial profile of the sound speed at the base of the convective zone and fail to predict the photospheric lithium abundance. In parallel, helioseismology has shown that the transition from differential rotation in the convective zone to almost uniform rotation in the radiative solar interior occurs in a shallow layer called the tachocline. This layer is presumably the seat of a large scale circulation and of turbulent motions. Here, we introduce a macroscopic transport term in the structure equations, which is based on a hydrodynamical description of the tachocline proposed by Spiegel & Zahn, and we calculate the mixing induced within this layer. We discuss the influence of different parameters that represent the tachocline thickness, the Brunt-Väissälä frequency at the base of the convective zone, and the time dependence of this mixing process along the Sun's evolution. We show that the introduction of such a process inhibits the microscopic diffusion by about 25 %. Starting from models including a pre-main sequence evolution, we obtain:

- a) a good agreement with observed photospheric chemical abundance of light elements such as ³He, ⁴He, ⁷Li and ⁹Be,
- b) a smooth composition gradient at the base of the convective zone, and
- c) a significant improvement of the sound speed square difference between the seismic Sun and the models in this transition region, when we allow the photospheric heavy element abundance to adjust, within the observational incertitude, due to the action of this mixing process.

The impact on neutrino predictions is also discussed.

Subject headings: Sun: interior, Sun: tachocline, Sun: oscillations, abundances, lithium, neutrinos

1. INTRODUCTION

The validation of solar structure is crucial to check the hypotheses used in stellar evolution modelling. It allows also the helium content at the birth of the Sun to be determined, which is key to galactic enrichment and for predicting the present neutrino emission fluxes. With the support of helioseismology, we are now able to constrain the sophisticated calculations performed to describe the present structure of the Sun. Very recently, a tremendous effort using ground based networks and space experiments has been made to improve the accuracy of the seismic tool at a level where differences with the theoretical estimates are significant. Consequently, it has been demonstrated that this discipline has the potential to check classical stellar structure for solar-type stars in the hydro-

gen burning phase (Tomczyk et al. 1995, Kosovishev et al. 1997, Turck-Chièze et al. 1997, Christensen-Dalsgaard 1998...).

In parallel, the development of neutrino detectors in particle physics has the objective of determining the properties of these particles. In this research, the Sun plays, once again, a specific role as a source of electronic neutrinos ν_e which could be transformed into other flavors before reaching the detectors on Earth (Hata & Langacker 1997, Bahcall, Krastev & Smirnov 1998). The solar conditions are really inaccessible in experiments on Earth, so one must predict precisely the emitted neutrino fluxes in order to progress in our knowledge of these particles and the solar core.

At first glance, helioseismology shows that the stan-

standard solar framework is correct (Brun, Turck-Chièze & Morel 1998; hereafter paper I). It is nevertheless extremely clear that standard models have always failed to answer some well known questions or anomalies due to its simplified assumptions (Turck-Chièze et al. 1993). These open questions concern the effect of the rotation and magnetic field, the history of the angular momentum, the real way the convection acts, the unexplained photospheric abundances as the photospheric lithium depletion and the presence of mixing at different locations inside the stars. Recent results obtained with the SOHO satellite (Fröhlich et al., 1997, Kosovishev et al. 1997, Gabriel et al. 1997) and ground networks have demonstrated that there exists significant differences in the square of the sound speed between the Sun and the models (Kosovishev et al. 1997, Turck-Chièze et al. 1997). Some of them can be attributed to uncertainties in the microscopic description of the Sun, while some others must be the sign of missing processes in the standard solar framework.

The idea of this paper is to introduce a new term in the stellar structure equations in order to progress beyond the standard framework. This new term describes some physical processes which are presumably present in our star as suggested by the differential rotation profile. In this study, we hope to treat more correctly the transition layer between the convective and radiative zones, with the help of crucial measured helioseismic variables. The main reasons for our interest in this layer are:

- The change of rotation rate (solid \Rightarrow differential) measured by helioseismology (Thompson et al. 1996, Kosovichev et al. 1997) develops probably some turbulent mixing in a shallow layer (tachocline) which could be where the magnetic field is anchored and amplified by dynamo process (Schüssler 1987, Choudhuri, Schüssler & Dikpati 1997),
- The fact that the standard solar model framework including microscopic diffusion and element settling has failed to treat this transition correctly (paper I). Such a model leads to sharp element profiles which create a large bump in the sound speed profile below the convective zone and cannot reproduce the observed lithium depletion,
- The turbulent convective zone surely interacts with the stably stratified radiative zone (e.g the Brunt-Väisälä frequency $N^2 > 0$), developing turbulence, modifying the thermal structure of the star (convective penetration) (Zahn 1991), or extending the mixing zone (overshooting)

(Roxburgh 1997 and Zahn 1998) or generating internal waves (Press 1981, Schatzman 1993).

Following the description of Spiegel & Zahn (1992) (hereafter; SZ92) of the motions in this so-called tachocline and that of Chaboyer & Zahn (1992) for the chemical evolution, we introduce in the equations of the stellar structure an effective diffusion coefficient and build several solar models, which are compared to the helioseismic and surface abundance observations.

We first present in section 2 the physical model of the solar tachocline we use and deduce the vertical macroscopic diffusion coefficient to be introduced in the time evolution equation of the chemical abundances. Then in section 3 we present solar models with a mixing occurring in the tachocline, its impact on photospheric abundances, especially for lithium and beryllium and discuss the effect of the time evolution of such a mixing from the Sun early phases until the present days. In section 4 we comment our results on the changes observed in the sound speed profile, on the role of the solar composition and the recent nuclear reaction rates and on neutrino predictions. Finally we conclude in section 5.

2. THE SOLAR TACHOCLINE

The Sun is generally assumed to be in hydrostatic and thermal equilibrium, neglecting the effects of rotation and magnetic field. However, models built with these simplifying assumptions do not totally agree with the helioseismic data, in particular with those obtained by the satellite SOHO. It appears that macroscopic mixing processes must be taken into account not only in the convective zone, but also in the radiative interior. Macroscopic mixing may be introduced in the solar models by adding an effective diffusivity D_T in the equation governing the time evolution of the chemical species X_i . The equation becomes:

$$\frac{\partial X_i}{\partial t} = -\frac{\partial(4\pi\rho r^2 X_i V_i)}{\partial m} + \text{nuclear terms}, \quad (1)$$

where the velocity V_i of species i with respect to the center of mass is:

$$V_i = -4\pi\rho r^2 (D_i + D_T) \frac{\partial \ln X_i}{\partial m} + v_i. \quad (2)$$

The velocity V_i is the sum of a term which depends on the concentration gradient and another which does not, v_i (Burgers 1969, Proffitt & Michaud 1991). In this paper, we add a macroscopic diffusion term D_T to the microscopic diffusion term D_i . This will describe the mixing occurring in the shear

layer connecting the differential rotation in the convection zone to the solid rotation in the radiative interior. As presented in SZ92, a possible physical interpretation of this tachocline is obtained by invoking anisotropic turbulence with much stronger viscous transport in the horizontal than in the vertical direction (i.e $\nu_H \gg \nu_V$). Such turbulence reduces the differential rotation and therefore inhibits the spread of the layer deep inside the radiative zone, leading to a stationary state. For a justification of this anisotropy, we refer to Michaud & Zahn (1998).

2.1. The hydrodynamical description

The conservation of mass, momentum and entropy is given by:

$$\frac{\partial \rho}{\partial t} + \vec{\nabla} \cdot (\rho \vec{V}) = 0 \quad (3)$$

$$\rho \left(\frac{\partial \vec{V}}{\partial t} + (\vec{V} \cdot \vec{\nabla}) \vec{V} + 2\vec{\Omega} \wedge \vec{V} + \vec{\Omega} \wedge \vec{r} \right) = -\vec{\nabla} P - \rho \vec{\nabla} \Phi + \vec{\nabla} \cdot \|\tau\| \quad (4)$$

$$\rho T \left(\frac{\partial}{\partial t} + \vec{V} \cdot \vec{\nabla} \right) S = \vec{\nabla} \cdot (\chi \vec{\nabla} T) \quad (5)$$

where ρ is the density, P the pressure, T the temperature, $\vec{V} = (u, v, r\hat{\Omega} \sin \theta)$ is the local velocity in the rotating frame $\vec{\Omega}$. In this expression, the differential rotation $\hat{\Omega}$ appears explicitly, S is the specific entropy, $\|\tau\|$ the viscous stress tensor and Φ the gravitational potential. In order to ease the solution of this system of equations, some simplifying assumptions were made by SZ92, mainly:

- velocities are small compared to the sound speed: $\partial \rho / \partial t$ is negligible (anelastic approximation),
- advection terms and viscous forces are small compared to the Coriolis acceleration (i.e small Rossby and Ekman numbers),
- the tachocline is thin compared to the pressure scale height and the turbulent horizontal viscosity is stronger than the vertical one (i.e $\nu_H \gg \nu_V$).

After separating each variable into its mean value on the sphere plus a perturbation, e.g. $T(r, t) + \hat{T}(r, \theta, t)$, the linearized form of the equations in a stationary state is given by SZ92. Spiegel and Zahn define a streamfunction Ψ for the meridional flows by:

$$r^2 \rho u = \frac{\partial \Psi}{\partial x}, \quad r \rho v \sin \theta = \frac{\partial \Psi}{\partial r} \quad (6)$$

where $x = \cos \theta$, and project the variables of the equations describing the tachocline on horizontal eigenfunctions F_i :

$$\begin{aligned} (\hat{P}, \hat{T}, u) &= \sum_i (\tilde{P}_i, \tilde{T}_i, u_i) F_i(x) \\ \Psi &= \sum_i \tilde{\Psi}_i \int F_i(x) dx \\ x \hat{\Omega} &= \sum_i \tilde{\Omega}_i \frac{dF_i}{dx}. \end{aligned} \quad (7)$$

The dominant term for the even eigenfunctions is $i = 4$, but we will consider in our calculation even terms up to $i = 8$. From this projection, SZ92 deduce a fourth-order differential equation for the modal function $\tilde{\Omega}_i(r)$, defined in eq (7):

$$\frac{4\Omega^2}{\mu_i^4} \frac{1}{\rho \nu_H} \frac{\partial}{\partial r} \left\{ \frac{g}{N^2 c_p T} \frac{\partial}{\partial r} \left[\chi r^2 \frac{\partial}{\partial r} \left(\frac{T}{\rho g} \frac{\partial}{\partial r} \rho r^2 \tilde{\Omega}_i \right) \right] \right\} + \tilde{\Omega}_i = 0. \quad (8)$$

where μ_i are eigenvalues related to the eigenfunctions F_i (for $i = 4$, $\mu_4 = 4.933$), $\chi = 16\sigma T^3 / 3\kappa\rho$ is the radiative conductivity, N the Brunt-Väisälä frequency, Ω the mean rotation rate of the radiation zone, and all the other variables have their usual meaning.

The problem is simplified by treating the tachocline as a boundary layer in which the rapidly varying quantity is $\tilde{\Omega}_i$ and all the other physical quantities are assumed constant. By doing so, an analytical solution of the simplified fourth-order differential equation is (for simplicity we only give the expression for the modal index $i = 4$):

$$\tilde{\Omega}_4(\zeta) = \tilde{\Omega}_4(0) \sqrt{2} \exp(-\zeta) \cos(\zeta - \pi/4) \quad (9)$$

where $\tilde{\Omega}_i(0) = Q_i \Omega$, Q_i are numerical coefficients depending on the latitudinal variation of the differential rotation and we have defined a non dimensional depth:

$$\zeta = \mu_i (r_{bcz} - r) / d \quad (10)$$

with,

$$d = r_{bcz} (2\Omega/N)^{1/2} (4K/\nu_H)^{1/4} \quad (11)$$

being a parameter related to the tachocline thickness h , r_{bcz} the radius and $K = \chi / \rho c_p$ the radiative diffusivity, at the base of the convective zone.

With the latitudinal dependence of the angular velocity at the base of the convection zone borrowed from Thompson et al. (1996): $\Omega_{bcz} / 2\pi = 456 - 72x^2 - 42x^4$ nHz, we have reestimated the coefficient $Q_4 = -1.707 \times 10^{-2}$, as well as the ratio between the rotation rate of the radiative zone and the equatorial rate: $\Omega / \Omega_0 = 0.9104$. The prediction by Gough & Sekii (1997), who consider instead the magnetic

stresses, is ~ 0.96 ; presently, the seismic observations suggest a rotational ratio of 0.94 ± 0.01 (Corbard et al. 1999), which is intermediate between these two theoretical estimates.

The inversion of the rotational profile from helioseismology observations gives the width of the tachocline and its location below the convection zone. For a comparison between the observational thickness and the theoretical one, we have to consider the first zero of equation (9), e.g $h = 3\pi d/4\mu_4 \sim d/2$. The parameter d is then approximately equal to $2h$. In the solar models of section 3, we will treat h (hence d) as an adjustable parameter, in order to agree with the helioseismic inversion of the tachocline thickness (Basu 1997, Charbonneau et al. 1998, Corbard et al. 1998, 1999).

Our purpose now is to obtain an analytical expression for the vertical velocity u . We already have an expression for the differential rotation, the next step is to connect u to $\hat{\Omega}$. From the conservation of the angular momentum, we find a relation between the stream function $\hat{\Psi}$ and the differential rotation $\hat{\Omega}$. By writing the streamfunction as $\tilde{\Psi}_i = \rho r^2 u_i$ and introducing the analytical expression of $\hat{\Omega}_i$ (eq 9), we finally obtain after integration, the radial dependence of u_i ; in the case of $i = 4$ we get:

$$u_4(\zeta) = \frac{1}{2} \frac{\nu_H d}{r_{bcz}^2} \mu_4^3 Q_4 \exp(-\zeta) \cos(\zeta). \quad (12)$$

From this equation (12), we shall derive an expression for the macroscopic diffusivity D_T of the motions occurring in the tachocline.

2.2. Macroscopic diffusion of chemical species

We determine in this section the influence of the mixing on the evolution of chemical species, using the expression for the vertical velocity amplitude u_i (eq. 12). The anisotropic diffusion, invoked by SZ92 to stop the spread of the tachocline deeper in the radiative zone, interferes with the advective transport of chemicals. Chaboyer & Zahn (1992) have shown that the result is a diffusive transport in the vertical direction, with an effective diffusivity given by:

$$D_T = \frac{r^2}{D_H} \sum_n \frac{U_n^2(r)}{n(n+1)(2n+1)} \quad (13)$$

where U_n are the coefficients of the expansion of the vertical component of the velocity u in Legendre polynomials. The eigenfunctions F_i introduced in section 2.1 may be projected on these Legendre polynomials, and to a good approximation one has (keeping only

the $n=4, 6$ and 8 terms)

$$D_T = \frac{r^2}{D_H} \left[\left(\frac{8}{3}\right)^2 \frac{u_4^2(r)}{180} + \left(\frac{16}{5}\right)^2 \frac{u_6^2(r)}{546} + \left(\frac{128}{35}\right)^2 \frac{u_8^2(r)}{1224} \right] \quad (14)$$

One reaches the following expression for the vertical diffusivity in replacing u_4 by equation (12) in equation (14), same for $n = 6$ and $n = 8$ (c.f Fig 1):

$$D_T(\zeta) = \frac{1}{180} \frac{1}{4} \left(\frac{8}{3}\right)^2 \nu_H \left(\frac{d}{r_{bcz}}\right)^2 \mu_4^6 Q_4^2 \times \exp(-2\zeta) \cos^2(\zeta) + \text{higher order terms.} \quad (15)$$

where ζ is the scaled vertical coordinate defined in equation (10).

In this expression, it is assumed that the horizontal component of the macroscopic diffusivity D_H is equal to the horizontal viscosity ν_H . This coefficient is then introduced in the diffusive part of the equation (1) for the time evolution of the chemical abundances X_i , and we could thus obtain solar models including a treatment of the tachocline. Fig 1 compares the different values of the macroscopic diffusivity for models discussed in the next section, to the microscopic diffusion (here represented as a horizontal solid line). The value of $10 \text{ cm}^2 \text{ s}^{-1}$ for D_i is deduced from the expression of Michaud & Proffitt (1993) for ${}^4\text{He}$, in the case of the reference solar model at the present age. It must be pointed out that in our calculation these microscopic diffusion coefficients as well as the microscopic velocity v_i are evaluated for all the chemical species present in our gaz mixture, and are not assumed constant (see paper I). The amplitude of $D_{4\text{He}}$ varies only by 10% in the range $[0.6, 0.72] R_\odot$ and doesn't change significantly with time. The oscillating behaviour of the macroscopic coefficient seen in Figure (1) reflects the sub cells structure of the tachocline and reduces the lithium depletion in comparison with a purely exponential coefficient by a factor $\sim 1.5-2$ and induces stages in the radial chemical composition profile (c.f 3.2 and Fig 2). The mixing in the tachocline thus depends on the following parameters, for a given model of the present Sun:

- the rotation rate Ω , a measured quantity;
- the differential rotation rate $\hat{\Omega}$ (or its projection Q_i) inferred from helioseismology;
- the Brunt-Väisälä frequency N , determined by the extent of convective penetration;
- the horizontal diffusivity ν_H , which presumably sides with the differential rotation rate.

There are at present no firm prescriptions available for N and ν_H , therefore we must consider these or

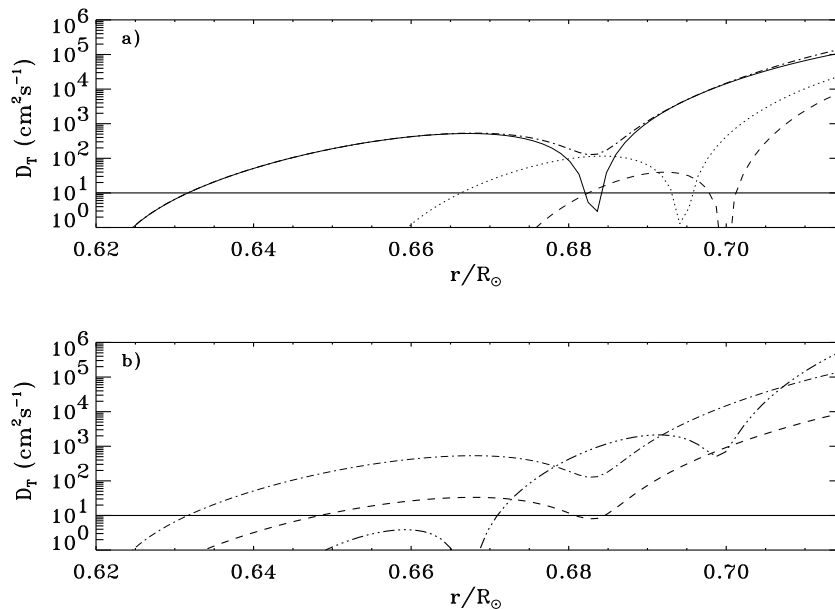


FIG. 1.— Effective diffusivity D_T for tachocline mixing: a) Model B ($N = 25$ and $d = 0.1$) for index $n = 4$ B_4 (solid line), $n = 6$ B_6 (...), $n = 8$ B_8 (- -) and $\sum_{n=4}^8 B_n$ (thick -.-). b) Models A ($N = 100$ and $d = 0.1$) (- -), B ($N = 25$ and $d = 0.1$) (-.-) and C ($N = 25$ and $d = 0.5$) (-.-.-). The horizontal solid line represents approximately the microscopic diffusion D_i .

two combinations of them, as free parameters in our calculations. We have chosen to keep N and to take d (twice the thickness of the tachocline), because both of them are constrained by upper limits drawn from helioseismology.

3. SOLAR MODELS

3.1. Description of the models

In paper I (Brun, Turck-Chièze & Morel 1998), we have calculated a new standard model using the CE-SAM code (Morel 1997) and have discussed the validity of such a model in the light of the present helioseismic observations. We just recall here the main physical inputs present in this reference model. We used the solar chemical composition of Grevesse, Noels & Sauval (1996), the OPAL96 opacity tables Iglesias & Rogers (1996) and the equation of state of Rogers, Swenson & Iglesias (1996), the recent updated nuclear reaction rates of Adelberger et al. (1998), the prescription of Mitler (1977) for the treatment of the nuclear screening reaction rates for a charge $Z > 2$ (Dzvitko et al., 1995) and the microscopic diffusion coefficients suggested by Michaud & Proffitt (1993).

In the present paper (called paper II), we use the “pure microscopic diffusion” model as the reference model. We then compute solar models using the macroscopic coefficient D_T described by equation (15) and follow the time evolution of these solar models from the pre-main sequence (PMS) until an age of 4.55 Gyr, making the age of our present Sun 4.6 Gyr (including about 0.05 Gyr of pre-main sequence). The adaptable time step increases from ~ 20 years up to 200 Myr during the evolution. We start from the

PMS so as to properly follow the ${}^7\text{Li}$ abundance evolution, including the macroscopic diffusion coefficient along all the solar phases. We introduced an updated nuclear reaction rate for ${}^7\text{Li}(p,\alpha){}^4\text{He}$, Engstler et al. (1992) instead of the Caughlan & Fowler (1988) one. The results of the solar models we calculated for this study are summarized in Tables 1 and 2 and the photospheric abundances of the elements which are sensitive to the adding macroscopic process are compared to observations in Table 3.

3.2. Time independent rotation

We first compute solar models including the effective diffusivity D_T (eq. 15), with a tachocline thickness h of $0.05 R_\odot$ ($d = 0.1 R_\odot$) in agreement with the helioseismic measurements (Basu 1997, Corbard et al. 1998, 1999, Charbonneau et al. 1998), a Brunt-Väissälä frequency N of 100 or 25 μHz to take into account the rapid variation of this quantity at the base of the convective zone, and a rotation Ω at the base of the convective zone of $0.415 \mu\text{Hz}$; we call these coefficients A and B respectively (see Table 1). The reference model has a present photospheric helium abundance of 0.2427 in mass, corresponding to an ${}^4\text{He}$ diffusion of 10.8%. This value of Y_s is slightly too low if we compare with the Basu & Antia (1995) value for the OPAL equation of state, $Y_s = 0.249 \pm 0.003$. When introducing the macroscopic diffusion coefficient, we mix back helium in the convection zone, inhibiting the microscopic diffusion by 15% or 25% and leading to a present photospheric ${}^4\text{He}$ abundance $Y_s = 0.2452$ or $Y_s = 0.2473$ respectively for models A and B (c.f Tables 1 and 3, see also Brun, Turck-Chièze & Zahn 1998). This is in better agreement

with the helioseismic values. The decrease of the Brunt-Väisälä frequency N leads to an increase of the efficiency of the mixing in the tachocline layer and reduces the settling of the chemical species. We also note that the initial helium content Y_0 is smaller than 0.27 in mass (cf Table 1 and also paper I).

In Figure 2 we present the difference between the initial helium composition Y_0 and the present photospheric one Y_s for several models including the reference one. Before the introduction of microscopic diffusion, this difference was null because the present photospheric values were adopted as the initial composition of the star. However now, when we compute a standard model including the microscopic diffusion and the settling of chemical species, the initial abundances are assumed to be different from their present day values and there is an iteration on the composition to get the photospheric Z/X ratio in agreement with the one measured at the present time: $Z/X = 0.0245 \pm 0.003$.

The prominent feature of Figure 2 is the smoother composition profile for models including the macroscopic diffusivity D_T , in comparison with the reference model, which presents a sharp composition gradient just below the convective zone. The composition profile is also almost constant below the convective zone over a distance which is related with the value of d and N . A smaller Brunt-Väisälä frequency value induces a greater mixing, and then an extended plateau. The characteristic steps in the radial profile come from the cosine term in the expression of D_T (eq. 15) (see also Elliott (1997)). An explanation could be that the simplified assumption in the treatment of the tachocline of SZ92, of a constant turbulent horizontal viscosity ν_H , induces this radial dependence of the coefficient D_T and thus the steps in the composition profile. A more careful study should be done to verify this statement.

Concerning the ${}^7\text{Li}$ and ${}^9\text{Be}$ depletion, we see in Table 3 that the mixing increases the lithium depletion by a factor up to ~ 4 , without burning ${}^9\text{Be}$, which agrees with the revised determination by Balachandran & Bell (1998). Nevertheless, such an increase of the ${}^7\text{Li}$ depletion is still insufficient to reproduce the photospheric lithium depletion (Grevesse, Noels & Sauval 1996, Cayrel 1998 and references therein).

3.3. Time dependent rotation

In this section we shall take into account the time evolution of the tachocline width and the efficiency of the mixing from the early phase of the Sun until now. In the previous section, we have used a constant value for d based on the present observations of the tachocline thickness in the effective diffusion coefficient D_T . Thus, in order to improve the description

of tachocline mixing, we now introduce a time dependence of the coefficient D_T and of the tachocline thickness h (hence d), related to the global and the differential rotation of the Sun as follows:

$$D_T \propto \nu_H \left(\frac{d}{r_{bcz}} \right)^2 Q_i^2 \propto \Omega \nu_H^{1/2} (\hat{\Omega}/\Omega)^2, \quad d \propto \Omega^{1/2} / \nu_H^{1/4}, \quad (16)$$

where we have used equations (15) and (11). Assuming that the turbulent viscosity is proportional to the differential rotation (i.e $\nu_H \propto \hat{\Omega}$) and introducing the dependence of differential rotation on rotation observed by Donahue, Saar & Baliunas (1996) ($\hat{\Omega} \propto \Omega^{0.7 \pm 0.1}$), we finally obtain for $D_T(\Omega)$ and $d(\Omega)$ the following scaling laws:

$$D_T \propto \Omega^{0.75 \pm 0.25}, \quad d \propto \Omega^{(1.3 \mp 0.1)/4}. \quad (17)$$

We conclude that the tachocline mixing was stronger in the past both because that layer was thicker and because the diffusivity was larger. Note that the observational uncertainties in the relation between $\hat{\Omega}$ and Ω act in opposite way on the dependence of $D_T(\Omega)$ and $d(\Omega)$ (i.e a stronger mixing implies a smaller tachocline extent). We render the mixing in the tachocline time-dependent, through $D_T(\Omega(t))$ and $d(\Omega(t))$, by using the spin-down law $\Omega(t) \propto t^{-1/2}$ which was deduced by Skumanich (1972) from the rotation rate of stellar clusters of different ages.

Models A_t , B_t and C_t correspond to solar evolutions with time-dependent coefficients given by equation (17) and different values for N and the present tachocline thickness d (see Table 1 and 2). The first two cases correspond to the same values of d and N that existed in the previous section but with a time dependence of the coefficient D_T . The third shows the influence of a thinner tachocline ($d = 0.05 R_\odot$) as suggested by more recent studies (Corbard et al. 1999). The introduction of this time-dependence increases the inhibition of the microscopic diffusion of helium during the evolution in comparison with the previous solar models considered in section 3.2 (see Table 3). These models show an inhibition of ${}^4\text{He}$ up to 27% for model B_t ($d = 0.1$, $N = 25$) leading to a surface helium $Y_s = 0.2477$, very close to the seismic value of Basu & Antia (1995).

We plot the ${}^7\text{Li}$ and ${}^9\text{Be}$ radial profiles in Figure 3, for the reference model and the time dependent models calibrated in Z/X at 4.6 Gyr, with the corresponding radial temperature scale. These two light chemical elements are sensitive to mixing processes occurring in the stars because their nuclear burning temperatures are very low (resp. $2.5 \cdot 10^6$ and $3.2 \cdot 10^6$ K) (Baglin & Lebreton 1990). It is well known that the solar ${}^7\text{Li}$ is depleted by a factor ~ 100 (Grevesse, Noels & Sauval 1996) and recent revised abundance

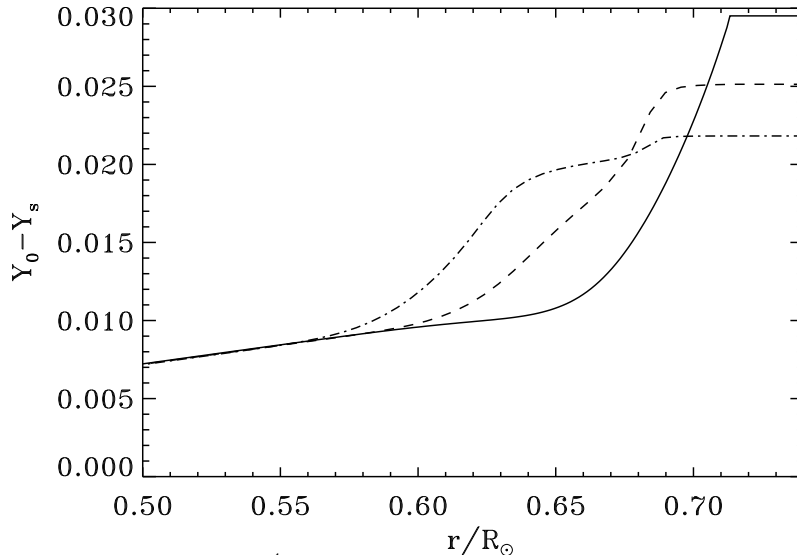


FIG. 2.— Radial profile of the difference of ${}^4\text{He}$ composition between the initial and present values for the reference solar model including only microscopic diffusion (solid line) and solar models where we add a macroscopic mixing due to the presence of the tachocline: coefficient A (- -) and B (-.-) (see section 3.3 and Tables 1, 3 for the model characteristics).

determinations have shown that ${}^9\text{Be}$ abundance is practically not depleted (Balachandran & Bell 1998) contrary to what was thought previously. These new observational constraints can only be satisfied if those chemical species are mixed in a rather thin layer below the convective zone, which is the case for the tachocline mixing considered here.

We clearly see in Figure 3 that this mixing process modifies the distribution of lithium but not of beryllium (except the flat plateau for the mixed models in comparison with the “pure” diffusion one). These results are confirmed in Table 3 where we show the initial over present ratio of the ${}^7\text{Li}$ and ${}^9\text{Be}$. We also remark that models including a macroscopic diffusivity with a low value of the Brunt-Väisälä frequency $N = 25$ (i.e B_t and C_t) burn more ${}^7\text{Li}$, because of their higher absolute value ($\geq 10^5 \text{ cm}^2\text{s}^{-1}$) in comparison with the microscopic diffusion one ($\sim 10 \text{ cm}^2\text{s}^{-1}$), than models with a higher $N = 100$ (i.e A_t) (Figure 1). The models B_t and C_t strongly inhibit the settling of the chemical species and mix all the elements over a distance where the lithium burning temperatures are reached $r \sim 0.67R_\odot$. The characteristic time for this mixing, for a D_T of $10^5 \text{ cm}^2\text{s}^{-1}$ is ~ 3 Myr. This time is intermediate between the convective cell turnover time (~ 1 month) and the microscopic diffusion one (> 10 Gyr). We also see in Table 3 that the time dependent diffusivity improves the ${}^7\text{Li}$ depletion, where a value of ~ 100 is obtained without destroying ${}^9\text{Be}$ and without increasing the ${}^3\text{He}/{}^4\text{He}$ surface ratio over the past 3 Gyr, as deduced by Geiss & Gloeckler (1998) from meteorites and solar wind abundance measurements. As already mentioned these abundance constraints can only be satisfied if the mixing occurs in a thin layer below the

convective zone, which is the case for the tachocline considered here.

In Figure 4 we present the lithium depletion occurring during the Sun evolution for the different models presented, plus one without microscopic diffusion. Clearly, only the diffusion models including mixing in the tachocline show a substantial depletion during the main sequence evolution as it is observed in different clusters. One notes that the lithium depletion is largely dependent on the Brunt Väisälä frequency adopted at the base of the convective zone and on the time dependence of the macroscopic coefficient. The modification of the tachocline thickness has only little impact on the lithium depletion as the higher value of the coefficient largely compensates the reduction of the thickness. However one sees that the ${}^7\text{Li}$ depletion slopes in these two models (i.e B_t and C_t) are not the same. The strong time dependent mixing with $N = 25$ presents a correct value of the solar ${}^7\text{Li}$ depletion. The lithium depletion during the PMS is probably overestimated due to the crude spin-down law we have adopted. A more detailed analysis of these phases is under study (see also Vauclair & Richard 1998 and Montalbán & Schatzman 1996).

4. DISCUSSION

4.1. The sound speed profile

We now compare the sound speed profile of the different models with the helioseismic inversion results obtained with the GOLF+MDI data (Lazrek et al. 1997, Roca Cortes et al. 1998, Kosovishv et al. 1997) and described in Turck-Chièze et al. (1997, 1998) (Fig 5), we see that the peak localized at $r \sim 0.68R_\odot$ is practically erased by this process, depending on the strength of the mixing.

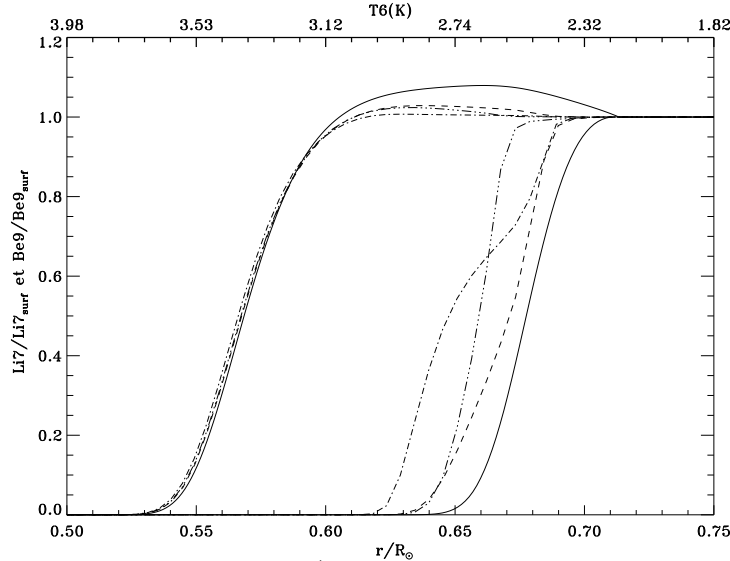


FIG. 3.— ${}^7\text{Li}$ and ${}^9\text{Be}$ radial profile for several models (superimposed the corresponding temperature $T_6 = T/10^6$ K obtained for the reference model). Respectively: reference (solid line), models A_t (dash), B_t (dash dot) and C_t (dash three dots). The mixing below the convective zone modifies only the ${}^7\text{Li}$ profile and not the ${}^9\text{Be}$ one (except the flat plateau for the mixed models).

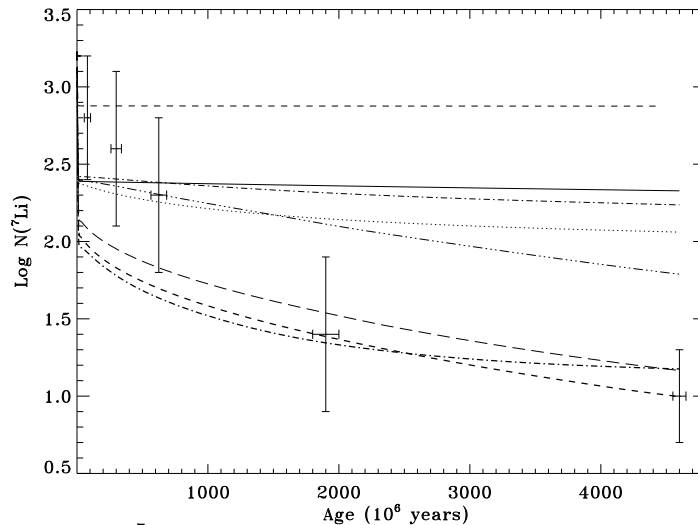


FIG. 4.— Time dependent depletion of ${}^7\text{Li}$ for several solar models: no microscopic diffusion (---), with microscopic diffusion (solid line) and with mixing in the tachocline thickness: models A (-.-), B (-...-), then with time dependent mixing, models A_t (...) and B_t (long dash), C_t (thick -.-) and B_{tz} ($Z_0 = Z_0^{std} = 0.01959$) (thick -.-). We superimposed on the theoretical curves the open cluster observations: (αPer : Balachandran et al. (1996); Pleiades: Soderblom et al. (1993b); UMaG: Soderblom et al. (1993a); Hyades: Thorburn et al. (1993); NGC752: Balachandran (1995). (Figure adapted from Vauclair & Richard 1998 and cluster age uncertainties deduced from Lebreton et al. 1997 and private communication.)

In all the models shown in this figure (5), we have adjusted the initial composition in order to get at the solar age, the present observed photospheric heavy element/hydrogen ratio, i.e $Z/X=0.0245$. This calibration causes the swell of the small bump located between the nuclear core and the convective zone, since it reduces the initial metallicity (see Table 2). It is well known that the heavy element abundance has a direct influence on the solar structure, mainly through the opacity coefficients and hence it influences the sound speed profile between 0.4 and $0.7 R_\odot$ (Turck-Chièze 1995, 1998 and paper I). The result is quite different if we do not constrain the photo-

spheric Z/X value of the mixed model, starting with the heavy element composition $Z_0 = 0.01959$ of the reference model for example, we obtain a different chemical composition at the solar age (see for example columns 3 and 4 of Table 2 for the coefficients B_t and B_{tz}). In Figure 6, we draw the corresponding squared radial sound speed differences between the models and the induced solar value for two models where we have kept (i.e coefficient B_t) or relax (B_{tz}) this surface heavy element constraint. We see that in both cases where the macroscopic term is introduced, the bump around $0.68 R_\odot$ is practically erased by the introduction of the tachocline mixing, but the cali-

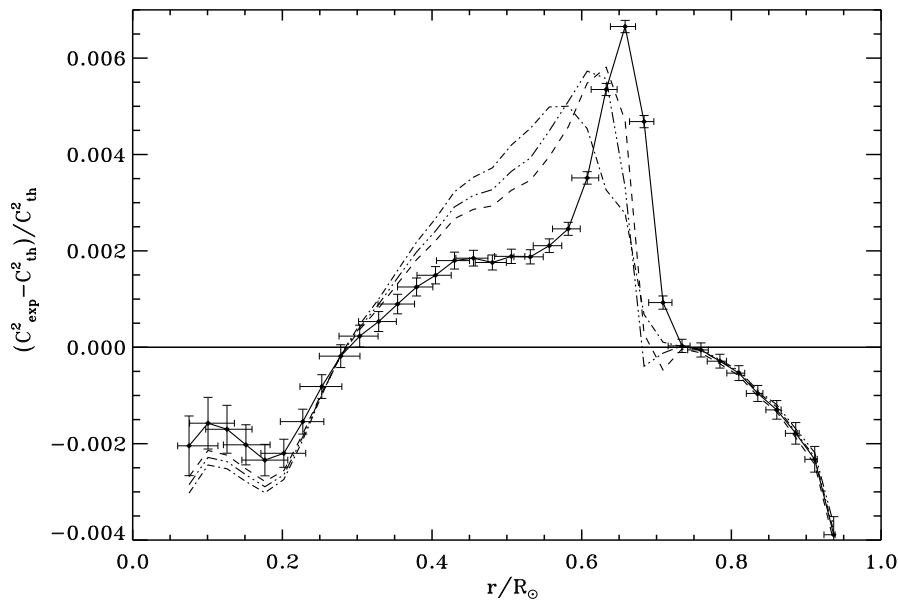


FIG. 5.— Sound speed square difference between GOLF+MDI data, the reference model (solid line) and models including a macroscopic term: A_t (---), B_t (---), C_t (-.-.) (see parameters in Table 2).

brated model is modified along the whole structure and not only close to the bump. It is not the case for the non-calibrated model where Z_0 is fixed. This is partly illustrated by Figure 7a, where the non-calibrated model changes only locally the structure of the solar model (dash dot line).

A similar result is obtained by Elliott, Gough & Sekii (1998) invoking an advection of the heavy elements at the base of the convection zone. They deduced from the sound speed profile a low value of the tachocline thickness ($h = 0.02$) which could be due to the macroscopic coefficient used. In this estimate, they did not calibrate their model in Z/X and obtained a result similar to ours (dash dot line in figure 7a).

4.2. Solar composition

Examining the different observables, it seems that the model using the coefficient B_{tz} (see Tables 2 and 3) corresponds today to a good representation of the present Sun. The agreement on the sound speed is significantly improved and the observed photospheric light elements (^3He , ^4He , ^7Li , ^9Be) are well reproduced. In this model, two effects contribute to this improvement; the introduction of the mixing at the base of the convection zone, which partly inhibits the microscopic diffusion, and the induced increase of the heavy elements at the surface and consequently in the intermediate region due to this inhibition. This model treats the tachocline instability as a local phenomenon.

In Figure 7b we show the heavy element profile along the solar radius of the reference model and the mixed models (coefficients B_t & B_{tz}) with and without the $Z/X=0.0245$ calibration. We clearly see

that without the Z/X calibration there is a difference in the Z profile, corresponding to an increase of the opacity and then to a reduction of the disagreement between the seismic sound speed and the theoretical one.

In paper I, we had already mentioned that the sound speed difference between the Sun and the model may suggest that a slight increase of the heavy element composition of about 5% is required. One notes that the results we obtain without specific calibration but keeping the initial heavy element composition of the reference model, lead to a photospheric heavy element composition of $Z/X=0.0255$. This is still consistent with the present observational uncertainties (about 10%) even if a very recent work seems to suggest a possible reduction of the CNO abundances rather than an slight increase (Grevesse & Sauval 1998). We have verified this statement by performing a “pure” microscopic model with $Z/X=0.0255$. If one compares the sound speed profile of model B_{tz} (dot dash line) to the reference model with $Z/X=0.0245$ (Fig 6), it shows a better overall agreement with the seismic data. Otherwise, if one compares this model to a “pure” microscopic model with $Z/X=0.0255$, one reaches a different conclusion for the radiative part (identical to the comparison of model B_t with the reference model Fig 6). This intricate process shows that it is not so easy to find the real behaviour of the Sun. If we increase the initial heavy element abundance a little more, we destroy the agreement of the tachocline region and obtain a photospheric composition which is not in a good agreement with the present observations. So extensive studies are surely useful to properly disen-

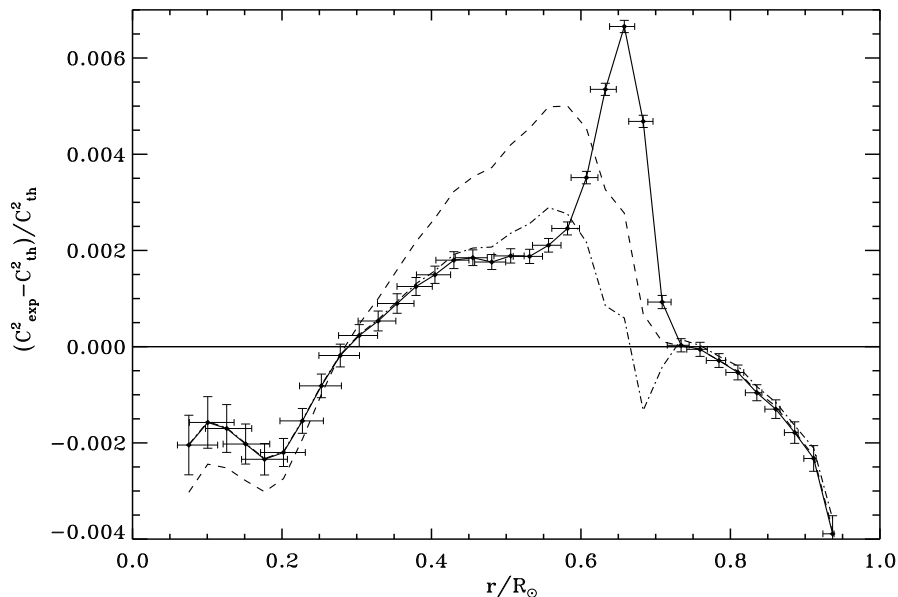


FIG. 6.— Sound square speed difference between GOLF+MDI data, the reference model (solid line) and two models including a macroscopic term: B_t calibrated in Z/X (- -) and B_{tz} with a non calibrated $Z_0 = Z_0^{std} = 0.01959$ (-.-).

tangle the competing processes.

The remaining part of the sound speed discrepancy located between the nuclear core and the convection zone (see Fig 6) may come from uncertainties in the equation of state or opacity coefficients (Turck-Chièze et al. 1998), or from our simplified treatment of the microscopic diffusion. In the present study, we do not consider the different states of ionisation of the different species or the radiative acceleration in the calculation of the microscopic diffusivity (Turcotte et al. 1998). We also cannot exclude the presence of other mixing processes, for example, the meridional circulation or the effect of the internal waves or magnetic field. It seems difficult to think that the residual discrepancy comes from insufficient knowledge of the element abundances, as an increase of the heavy element composition will have a dramatic effect in the region of the energy transport transition.

4.3. Nuclear reaction rates

The depletion of lithium is of course dependent on the nuclear reaction rates used. In this study, we have used the recent compilation of the NACRE consortium (Angulo et al. 1999), which recommends the nuclear reaction rate ${}^7\text{Li}(p,\alpha){}^4\text{He}$ of Engstler et al. (1992). The astrophysical factor is increased by 30% in comparison with the older value recommended by Caughlan & Fowler (1988), mainly due to a higher accuracy numerical integration. The updated value of $S_{71}(0) = 0.0593$ Mev barn increases the lithium depletion during the Sun evolution by $\sim 40\%$ (see Table 3 model B_{to} and B_t). This effect is introduced in all the results presented in this study and constitutes an important point which must be considered in the

lithium depletion problem in stars. It is interesting also to notice that the reaction rate of the ${}^7\text{Li}(p,\gamma){}^8\text{B}$ which is not included in our study, mainly because this cross section was considered as very small, has been reestimated these last years and found 100 times greater than in Caughlan & Fowler (1988). The impact on the present study must be smaller than 10%, considering the relative importance of the two reactions.

4.4. Neutrino predictions

Of course, one issue of improving solar models is to predict more correctly the neutrino fluxes produced in the central region of the Sun (Turck-Chièze 1999). Tables 1 and 2 show the predicted values for all the models considered. One notices a very small dependence on the macroscopic coefficient used, but nevertheless two kinds of results depending on whether the models are calibrated in Z/X or not. This difference is connected to the effect of the inhibition of the microscopic processes which leads to a slight decrease of the neutrino fluxes. Indeed, we observe, in the calibrated models, a reduction in comparison with the reference model of -1.6% for the Gallex and Sage experiments (resp. Hampel et al. 1996 and Abdurashitov et al. 1996), of -5.1% for the Homestake experiment (Cleveland et al. 1998) and -5.6% for SuperKamiokande (Suzuki et al. 1998). It is useful to recall that the general effect of the introduction of the microscopic diffusion in solar model was an increase of about 20% on the ${}^8\text{B}$ neutrino flux prediction, so this corresponds to 25% of this effect. But, one may also notice that the effect of inhibition could be exactly compensated by the effect of the increase of the

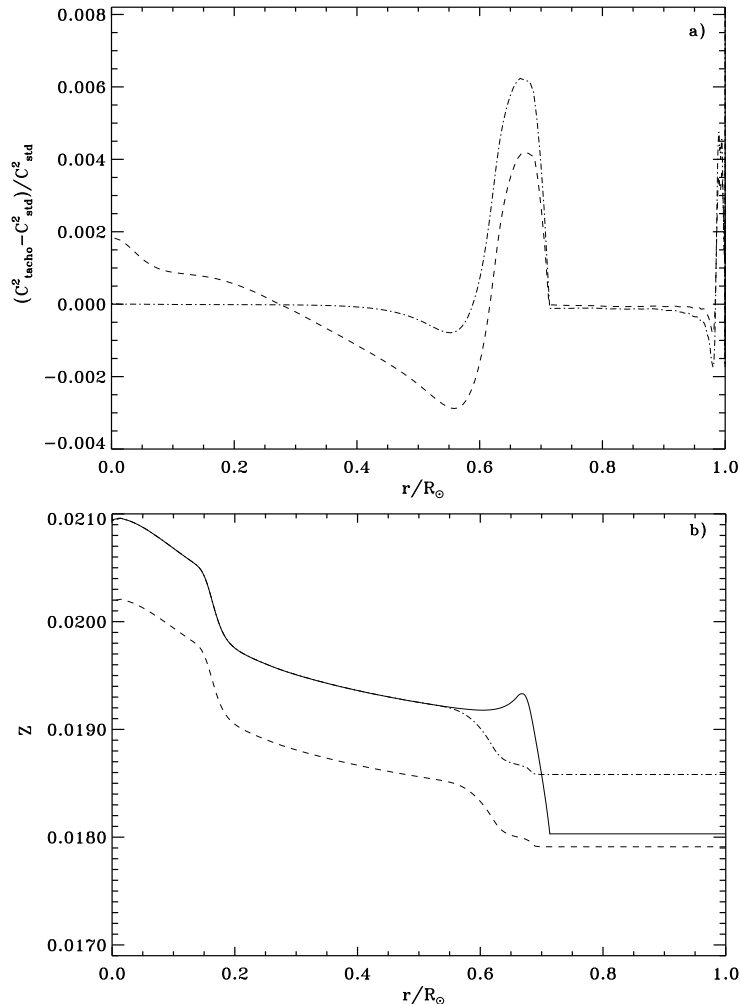


FIG. 7.— *a)* The effect of calibration on the sound square speed difference between the reference model and two models including a macroscopic term: B_t calibrated in Z/X (---) and B_{tz} with a non calibrated $Z_0 = Z_0^{std} = 0.01959$ (dash dot line). *b)* Heavy Element Composition for the reference model including only microscopic diffusion (solid line) and two models with macroscopic mixing due to the tachocline: B_t calibrated in Z/X (---) and B_{tz} with a non calibrated $Z_0 = Z_0^{std} = 0.01959$ (-.-). (see Table 2 for the model characteristics).

heavy elements by 5% (reference model and model B_{tz}).

These effects are too small to solve the neutrino problem. This is hardly a surprise, since the tachocline mixing occurs at the base of the convection zone, hence too remote to have a serious impact on the structure of the nuclear core. Even if this study is not crucial for the neutrino fluxes it gives certainly a proper description of the chemical transport of elements in the external part of the Sun and definitively excludes a large increase of the neutrino fluxes by this kind of processes as was thought five years ago. The introduction of a macroscopic diffusivity also destroys the criticisms on the impact of the pure microscopic diffusion which was well known to be partly inhibited by some turbulent processes and which seems now well under control, at least as far as the extension in the Sun is concerned. We begin to include dynamical effects properly in stellar

models and one cannot exclude that the cumulative effect of different modifications of the physical inputs (microscopic and macroscopic) may lead to smaller neutrino fluxes. We will not comment, in this paper, on the discrepancy of the sound speed in the central region because this is more difficult to estimate (Turck-Chièze & Basu 1998, Gonczi et al. 1998) and to interpret there, due to the sensitivity of the sound speed to a lot of competing processes (see paper I). Works are in progress to have good constraints on the core.

5. CONCLUSION

In this paper, we have shown that the presence of mixing in the tachocline layer partly inhibits the microscopic diffusion process and improves the agreement with the helioseismic and photospheric abundance data. Our results make use of updated helioseismic constraints on the present extent of this layer, and they are based on a physical treatment of

the tachocline layer (SZ92) which involves only one additional parameter, namely the Brunt-Väisälä frequency (which we assume constant in our model). The solar models thus obtained are quantitatively in good agreement with the observational data and our favoured model is model B_{tz} (cf. Tables 2 & 3). When introducing a time dependent tachocline mixing, it is possible to reach the observed ${}^7\text{Li}$ photospheric abundance at the present solar age, without destroying ${}^9\text{Be}$ or bringing too much ${}^3\text{He}$ at the surface. This does not necessarily mean that our mixing process is the only one which operates in the Sun: others may contribute, such as mixing by gravity waves (Montalban & Schatzman 1996) or meridional circulation (Zahn 1992, Vauclair & Richard 1998). But the lack of depletion of ${}^9\text{Be}$ proves that the mixing occurs in a rather thin layer below the convective zone, which is the case in our models. The model which seems the most promising assumes a Brunt-Väisälä frequency $N = 25\mu\text{Hz}$; it leads to a slight increase of the heavy element abundance by 5% at the surface, compatible with the present uncertainties. A detailed study of the feedback of such mixing on the structure of the Sun reveals that its effect is not confined to the base of the convection zone, but that it spreads into the region below, except if one relaxes the fixed Z/X constraint and let the model adjusts within the heavy element abundance uncertainties (model B_{tz}).

From the results of papers I and II, we could deduce a galactic enrichment of ${}^4\text{He}$. We find that the solar ${}^4\text{He}$ primordial abundance is $Y_0 = 0.27_{-0.001}^{+0.002}$ and leads to an enrichment of $10.6_{-1.3}^{+2.8}\%$ from the value of 0.244 ± 0.002 deduced by Thuan & Izotov (1998) from observations of a large sample of low-metallicity H II regions in blue compact dwarf galaxies.

This first attempt to calibrate dynamical processes with helioseismology data from SOHO leads to the idea that the neutrino problem could be seen from a new angle, by considering reliable solar models with macroscopic processes, never implemented previously. The process invoked here concerns the 5% part of the external mass and consequently has little impact on neutrino predictions. But, even if the solar models are close to the seismic data for $r < 0.2R_\odot$, the remaining discrepancies are still significant (\sim few σ) in comparison with seismic uncertainties, and they suggest that other physical processes, neglected so far, may operate there.

To conclude, this study encourages the introduction of new processes in stellar structure theory, beyond the standard model framework. Of course we are aware of the crudeness of the present model: a more refined treatment would include the variation with depth of the horizontal turbulent diffusivity and of the Brunt-Väisälä frequency, as well as a more precise spin-down law, and it would not ignore the magnetic field.

REFERENCES

- Abdurashitov et al. (SAGE collaboration), 1996, Phys. Rev. Lett., 77, 4708.
- Adelberger, E. et al. 1998, Rev. Mod. Phys., 70 (4), 1265.
- Angulo, C. et al., 1999, NACRE compilation, submitted.
- Alexander, D. R. & Ferguson, J. W. 1994, ApJ, 437, 849.
- Bahcall, J. N., Krastev, P. I. & Smirnov, A. Yu. 1998, hep-th/9807216.
- Baglin, A. & Lebreton, Y. 1990, Inside the Sun, eds G. Berthomieu & M. Cribier, Kluwer Academic Publishers, Netherlands, 437.
- Balachandran, S. 1995, ApJ, 446, 203.
- Balachandran, S. Lambert, D. L. & Stauffer, J. R. 1996, ApJ, 470, 1243.
- Balachandran, S. & Bell, R. A. 1998, Nature, 392, 791.
- Basu, S., 1997, MNRAS, 288, 572.
- Basu, S. & Antia, H. M. 1995, MNRAS, 276, 1402.
- Burgers, J. M. 1969, Flow Equations for Composite Gases, Academic, New York.
- Brun, A. S., Turck-Chièze, S. & Morel, P. 1998, ApJ, 506, 913. (paper I).
- Brun, A. S., Turck-Chièze, S. & Zahn, J. P. 1998, in Structure and Dynamics of the Interior of the Sun and Sun-like Stars, eds S. G. Korzennik and A. Wilson, (ESA: Noordwijk), ESA SP-418, Vol 1, 439.
- Cayrel, R. 1998, Space Sci. Rev., 84, 145.
- Caughlan, G. R. & Fowler, W. A. 1988, Atomic Data and Nuclear Tables, 40, 284.
- Chaboyer, B. & Zahn, J. P. 1992, A&A, 253, 173.
- Charbonneau, P., Christensen-Dalsgaard J. & Henning, R., 1998, in Proceedings of IAU symposium 181, Nice, ed J. Provost & F.X. Smider, 161.
- Christensen-Dalsgaard, 1998, in Structure and Dynamics of the Interior of the Sun and Sun-like Stars, eds S. G. Korzennik and A. Wilson, (ESA: Noordwijk), ESA SP-418, vol 1, 17.
- Choudhuri, A. M., Schüssler, M. & Dikpati, M. 1997, A&A, 319, 362.
- Cleveland, B. T. et al. 1998, ApJ, 496, 505.
- Corbard, T., Berthomieu, G., Provost, J. & Morel, P. 1998, A&A, 330, 1149.
- Corbard, T., Blanc-Féraud, L., Berthomieu, G. & Provost, J. 1999, to appear in A&A.
- Donahue, R. A., Saar, S. H. & Baliunas, S. L. 1996, ApJ, 466, 384.
- Dzitko, H., Turck-Chièze, S., Delbourgo-Salvador, P., & Lagrange, G. 1995, ApJ., 447, 428.
- Elliott, J. R. 1997, A&A, 327, 1222.
- Elliott, J. R., Gough, D. O. & Sekii, T. 1998, in Structure and Dynamics of the Interior of the Sun and Sun-like Stars, eds S. G. Korzennik & A. Wilson, (ESA: Noordwijk), ESA SP-418, Vol 2, 763.
- Engstler et al. 1992, Phys. Rev. Lett. B, 279, 20.
- Fröhlich, C., et al., 1997, Sol. Phys., 170, 1.
- Gabriel et al., 1997, Sol. Phys., 175, (2), 207.
- Geiss, J. & Gloeckler, G. 1998, Space Sci. Rev., 84, 239.
- Gonczy, G., Berthomieu, G., Corbard, T., Provost, J., Morel, P. and the GOLF team, 1998, in Structure and Dynamics of the Interior of the Sun and Sun-like Stars, eds S. G. Korzennik and A. Wilson, (ESA: Noordwijk), ESA SP-418, vol 1, 461.
- Gough, D. O. & Sekii, T. 1997, IAU 181 Sounding Solar and Stellar Interior (poster volume), eds J. Provost and F. X. Smider, Observatoire de la Côte d'Azur, Nice.
- Grevesse, N., Noels, A., & Sauval, A. J. 1996, in Cosmic Abundances, ed. S. S. Holt and G. Sonneborn, ASP Conference Series, 117.

- Grevesse, N., Sauval, A. J., 1998, *Space Sci. Rev.*, 85, 161.
- Hampel, W. et al. (GALLEX collaboration), 1996, *Phys. Lett.* B388, 384.
- Hata, N. & Langacker, P. 1997, hep-ph/9705339.
- Iglesias, C. & Rogers, F. J. 1996, *ApJ*, 464, 943.
- Kosovichev, A. G., et al., 1997, *Sol. Phys.*, 170, 43.
- Lebreton Y., Gomez, A.E., Mermilliod, J.-C., Perryman, M.A.C. 1997, in Proceedings of the ESA Symposium 'Hipparcos- Venice '97', ESA SP-402, 231.
- Michaud, G. & Proffitt, C.R. 1993, *Inside the stars IAU 137*, ed. W. W. Weiss & A. Baglin (ASP: San Francisco), 246.
- Michaud, G. & Zahn, J.-P. 1998, *Theoret. Comput. Fluid Dynamics*, 11, 183.
- Mitler, H. E. 1977, *ApJ*, 212, 513.
- Montalban, J. & Schatzman, E. 1996, *A&A*, 305, 513.
- Morel, P. 1997, *A&A Sup.*, 124, 597.
- Press, W. H. 1981, *ApJ*, 245, 286.
- Proffitt, C. R. & Michaud, G. 1991, *ApJ*, 380, 238.
- Roca-Cortés, T. et al., 1998, in *Structure and Dynamics of the Interior of the Sun and Sun-like Stars*, eds S. G. Korzennik and A. Wilson, (ESA: Noordwijk), ESA SP-418, vol 1, 329.
- Rogers, F. J., Swenson, J. & Iglesias, C. 1996, *ApJ*, 456, 902.
- Roxburgh, I. , 1997, in *SCORe'96*, eds F.P Pijpers, J. Christensen-Dalsgaard & C. S. Rosenthal, Kluwer Academic Publisher.
- Schatzman, E. 1993, *A&A*, 279, 431.
- Schüssler, M. 1987, *The Internal Solar Angular Velocity*, eds B. R. Durney & S. Sofia, Reidel Publishing Company, Dordrecht.
- Skumanich, A. 1972, *ApJ*, 171, 565.
- Soderblom, D. R., Pilachowski, C. A., Fedele, S. B. & Jones, B. F. 1993a, *AJ* 105, 2299.
- Soderblom, D. R., et al., 1993b, *AJ*, 106, 1059.
- Spiegel, E. A. & Zahn, J. P. 1992, *A&A*, 265, 106 (SZ92).
- Suzuki, Y. et al. 1998 (SuperKamiokande Collaboration), in *Neutrino 98*, Proceedings of the XVIII International Conference on Neutrino Physics and Astrophysics, Takayama, Japan, eds. Y. Suzuki & Y. Totsuka.
- Thompson, M. J., Toomre, J. and the GONG Dynamics Inversion Team 1996, *Sci*, 272, 1300.
- Thorburn, J. A., Hobbs, L. H., Deliyannis, C. P. & Pinsonneault, M. H. 1993, *ApJ*, 415, 150.
- Thuan, T. X. & Izotov, Y. I. 1998, *Space Sci. Rev.*, 84, 83.
- Tomczyk, S., Streander, K., Card, G., Elmore, D., Hull, H., & Cacciani, A. 1995, *Sol. Phys.*, 159, 1.
- Turcotte, S. et al., 1998, *ApJ.*, 504, 539.
- Turck-Chièze, S., et al., 1993, *Phys. Rep.*, 230 (2-4), 57.
- Turck-Chièze, S. 1995, *Adv. Space. Res.*, 15, 85.
- Turck-Chièze, S. et al. 1997, *Sol. Phys.*, 175,247.
- Turck-Chièze, S. 1998a, *Space Science Rev.*, 85, 125.
- Turck-Chièze, S. 1999, to appear in *New Astronomy*.
- Turck-Chièze, S. et al. 1998, in *Structure and Dynamics of the Interior of the Sun and Sun-like Stars*, eds S. G. Korzennik and A. Wilson, (ESA: Noordwijk), ESA SP-418, vol 1, 555.
- Turck-Chièze, S. and Basu, S. 1998, in *Structure and Dynamics of the Interior of the Sun and Sun-like Stars*, eds S. G. Korzennik and A. Wilson, (ESA: Noordwijk), ESA SP-418, vol 1, 573.
- Vauclair, S. & Richard, O., 1998, in *Structure and Dynamics of the Interior of the Sun and Sun-like Stars*, eds S. G. Korzennik and A. Wilson, (ESA: Noordwijk), ESA SP-418, vol 1, 427.
- Zahn, J. P. 1991, *A&A*, 252, 179.
- Zahn, J. P. 1992, *A&A*, 265, 115.
- Zahn, J.-P. 1998, *Space Sci. Rev.*, 85, 79.

Table captions

Definition of the parameters used in Tables 1 and 2:

d : is twice the tachocline thickness h , N : Brunt-Väisälä frequency, α : mixing length parameter, Y_0 , Z_0 , $(Z/X)_0$: initial helium, heavy element and ratio heavy element on hydrogen, Y_s , Z_s , $(Z/X)_s$: idem for surface compositions, R_{bzc} , T_{bzc} are the radius and temperature at the base of the convective zone, Y_c , Z_c , T_c , ρ_c : central helium, heavy element contents, central temperature and density, ^{71}Ga , ^{37}Cl , ^8B respective neutrino predictions for the gallium, the chlorine and water detectors. OPAL/A means that we use OPAL96 opacities and Alexander (1994) for low temperature.

TABLE 1

SOLAR MODELS WITH A TIME INDEPENDENT MACROSCOPIC DIFFUSIVITY DESCRIBING THE TACHOCLINE MIXING AND COMPARED TO THE REFERENCE MODEL, EACH OF THEM CORRESPONDS TO DIFFERENT VALUES OF THE BRUNT VÄISSÄLÄ FREQUENCY AND TO THE TACHOCLINE THICKNESS.

Parameters	Ref	A	B
Opacities	OPAL/A	OPAL/A	OPAL/A
Diffusion	yes	yes	yes
Age (Gyr)	4.6	4.6	4.6
d (r/R_\odot)	-	0.1	0.1
N (μHz)	-	100	25
$(Z/X)_s$	fixed	fixed	fixed
α	1.766	1.753	1.745
Y_0	0.2722	0.2703	0.2691
Z_0	0.01959	0.01919	0.01893
$(Z/X)_0$	0.0277	0.0270	0.0266
Y_s	0.2427	0.2452	0.2473
Z_s	0.01803	0.01797	0.01792
$(Z/X)_s$	0.0245	0.0245	0.0245
R_{bzc}/R_\odot	0.7133	0.7145	0.7154
$T_{bzc} \times 10^6$ (K)	2.190	2.181	2.174
Y_c	0.6405	0.6382	0.6367
Z_c	0.02094	0.02051	0.02024
$T_c \times 10^6$ (K)	15.71	15.68	15.66
ρ_c (g/cm^3)	153.1	152.9	152.7
^{71}Ga (SNU)	127.1	126.0	125.2
^{37}Cl (SNU)	7.04	6.84	6.71
^8B ($10^6/\text{cm}^2/\text{s}$)	4.99	4.83	4.73

TABLE 2

SOLAR MODELS WITH A TIME DEPENDENT MACROSCOPIC DIFFUSIVITY DESCRIBING THE TACHOCLINE MIXING AND COMPARED TO THE REFERENCE MODEL, EACH OF THEM CORRESPONDS TO DIFFERENT VALUES OF THE BRUNT VÄISSÄLÄ FREQUENCY AND TO THE TACHOCLINE THICKNESS, THE MODEL B_{tz} SHOWS THE EFFECT OF NON CALIBRATED Z/X (SEE TEXT).

Parameters	Ref	A_t	B_t	B_{tz}	C_t
Opacities	OPAL/A	OPAL	OPAL/A	OPAL/A	OPAL/A
Diffusion	yes	yes	yes	yes	yes
Age (Gyr)	4.6	4.6	4.6	4.6	4.6
d (r/R_\odot)	-	0.1	0.1	0.1	0.05
N (μHz)	-	100	25	25	25
$(Z/X)_s$	fixed	fixed	fixed	free	fixed
α	1.766	1.752	1.743	1.755	1.748
Y_0	0.2722	0.2701	0.2689	0.2722	0.2695
Z_0	0.01959	0.01914	0.01889	0.01959	0.01903
$(Z/X)_0$	0.0277	0.0269	0.0265	0.0277	0.0267
Y_s	0.2427	0.2455	0.2477	0.2510	0.2464
Z_s	0.01803	0.01796	0.01791	0.01858	0.01794
$(Z/X)_s$	0.0245	0.0245	0.0245	0.0255	0.0245
R_{bzc}/R_\odot	0.7133	0.7146	0.7155	0.7141	0.715
$T_{bzc} \times 10^6$ (K)	2.190	2.180	2.173	2.194	2.177
Y_c	0.6405	0.6379	0.6365	0.6405	0.6372
Z_c	0.02094	0.02047	0.02019	0.02094	0.02034
$T_c \times 10^6$ (K)	15.71	15.67	15.65	15.71	15.66
ρ_c (g/cm^3)	153.1	152.8	152.7	153.1	152.8
^{71}Ga (SNU)	127.1	125.9	125.1	127.1	125.5
^{37}Cl (SNU)	7.04	6.82	6.69	7.04	6.76
^8B ($10^6/\text{cm}^2/\text{s}$)	4.99	4.81	4.70	4.99	4.76

TABLE 3

SURFACE ABUNDANCE VARIATION OF $^3\text{He}/^4\text{He}$ DURING THE LAST 3 GYR, SURFACE ABUNDANCES OF ^4He AND HEAVY ELEMENTS Z, AND ABUNDANCE RATIO INITIAL/SURFACE FOR ^7Li AND ^9Be FROM OBSERVATIONS AND FOR SOLAR MODELS AT THE SOLAR AGE (SUBSCRIPTS t FOR TIME DEPENDENT MODELS, tz FOR TIME DEPENDENT MODEL WITH $Z_0 = Z_0^{ref} = 0.01959$ AND to FOR TIME DEPENDENT MODEL WITH CAUGHLAN & FOWLER (1988) $^7\text{Li}(p,\alpha)^4\text{He}$ NUCLEAR REACTION RATE).

	Obs	Ref	A	B	A_t	B_t	B_{tz}	B_{to}	C_t
d (r/R_\odot)	≤ 0.1	-	0.1	0.1	0.1	0.1	0.1	0.1	0.05
N (μHz)	-	-	100	25	100	25	25	25	25
$(^3\text{He}/^4\text{He})_s$	max 10%	2.28%	2.14%	2.01%	2.11%	2.0%	2.02%	2.0%	2.07%
$^4\text{He}_s$	0.249 ± 0.003	0.2427	0.2452	0.2473	0.2455	0.2477	0.2509	0.2477	0.2464
$(Z/X)_s$	0.0245 ± 0.002	0.0245	0.0245	0.0245	0.0245	0.0245	0.0255	0.0245	0.0245
$^7\text{Li}_0/^7\text{Li}_s$	~ 100	~ 6	~ 8	~ 22	~ 12	~ 91	~ 134	~ 64	~ 89
$^9\text{Be}_0/^9\text{Be}_s$	1.10 ± 0.03	1.115	1.093	1.086	1.093	1.118	1.125	1.118	1.092